Preprints of the 21st IFAC World Congress (Virtual)
Berlin, Germany, July 12-17, 2020

A Model Predictive Control Scheme to Improve Performance of a Path-following Controller for Airborne Wind Energy

Manuel C.R.M. Fernandes * **Luís Tiago Paiva** *
Fernando A.C.C Fontes *

* *Systec-ISR, Faculdade de Engenharia, Universidade do Porto, 4200-465 Porto, Portugal (e-mail:* {mcrmf,ltpaiva,faf}@fe.up.pt*).*

Abstract: Airborne Wind Energy Systems involve, in most solution concepts, flying kites at high speeds on a pre-specified, crosswind, optimized path. We develop a heading angle controller, using Model Predictive Control (MPC) on top of a guidance logic control, to maintain the kite within the desired path. The computed MPC law is used to enhance an existing controller and is able to preserve its stabilizing properties. The performance of the overall scheme can only improve upon the one of the basis controller. The optimization problems involved in the MPC algorithm are solved in an efficient way since the optimizer starts from a feasible solution. Nevertheless, even when the optimizer fails to provide an adequate solution in time, a guaranteed stabilizing law is used.

Keywords: Model Predictive Control, Optimal Control, Nonlinear Control, Path-following, Aircraft Control, Airborne Wind Energy, Wind Power, Renewable Energy Systems.

1. INTRODUCTION

We address Airborne Wind Energy Systems (AWES), in particular the problem of devising a control for the kite (tethered drone) to follow a pre-specified path. We propose a Model Predictive Control (MPC) scheme that is used to improve the performance of an existing path-following guidance method for AWES, maintaining its stability guarantees.

Airborne Wind Energy Systems are devices that convert wind energy into electricity using high speed flying wings attached to the ground by a tether. These systems aim to harvest wind energy at high altitudes, where the wind is stronger and more consistent, using a lightweight infrastructure (see e.g. Schmehl (2018)). AWES aim to exploit a huge, still unexploited resource – the high altitude winds –, having the potential to significantly contribute to the energy transition from fossil-based to renewable sources.

The development of a performant and robust path-following control scheme is timely and relevant for the advancement of AWES technology. On the one hand, in AWES, as in most electrical energy generation systems, maximizing output power production is a major goal. To achieve this goal, the kites should follow an optimized periodic path which can be found by solving an optimal control problem maximizing power production; see Houska and Diehl (2007); De Lellis et al. (2018); Paiva and Fontes (2018). The development of a controller that can closely follow the optimized path, as is proposed here, has a direct impact on the performance of the AWES. On the other hand, one of the main challenges towards the commercialization of AWES is to guarantee a safe, reliable and autonomous operation for long periods of time, under diverse weather conditions (see report van Hussen et al., 2018). The development of a controller that can guarantee convergence to a pre-specified path with a large domain of attraction, as is proposed here, contributes to this challenge.

In this paper, we use as basis a path-following guidance control law, which was shown to have global stabilizing properties (Silva et al., 2019). On top of such control law, we add a term computed within an MPC algorithm. The overall controller can only improve performance with respect to the basis controller. The objective functions for the optimal control problems involved in the MPC scheme are the Lyapunov control pair of functions that was used to verify the stability of the guidance control law. Therefore, it is guaranteed that the stabilizing properties are preserved (Fontes, 2001).

The heading angle control of kites in AWES has been previously studied in Fagiano (2009); Lellis et al. (2013); Silva et al. (2019), among others. The use of MPC on top of an already adequate stabilizing controller has been reported in the literature in (Magni et al., 2002; Zeiaee et al., 2017), on the control of an inverted pendulum and of a nonholonomic mobile robot, respectively. This complementary use of MPC brings about several advantages: (i) the stability of the MPC strategy can be guaranteed, by means of a constructive procedure to select stabilizing MPC design parameters; (ii) the performance of the combined controller can only improve upon the basis solution; (iii) the optimization problems within MPC strategy are numerically solved in a very efficient way, since the process already starts from a feasible solution; (iv) the method is robust even when the optimizer fails to provide an ade-

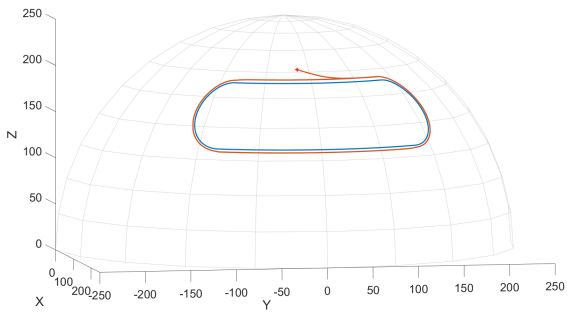

Fig. 1. Time–independent 3D path on the surface of a sphere (blue) and trajectory following it (red)

quate solution in time, since at least the feasible solution known from the beginning can be used.

2. PATH–FOLLOWING GUIDANCE AND CONTROL

2.1 Surface Path–following Parameterization

The maximization of power production is frequently a major goal in electrical energy generation systems. An approach to address this goal is to formulate it in an Optimal Control Problem (OCP) where the cost functional is set to maximize the power production. Such OCP can be solved using numerical methods and typically its solution is a periodic trajectory (Houska and Diehl, 2007; De Lellis et al., 2018; Paiva and Fontes, 2018). In real–time applications, instead of solving on–line a complete OCP, which would have a high computational cost, we implement a guidance scheme where the kite's trajectory has to follow a pre–specified path.

To design such time–independent 3D path (see Fig. 1), we start with the 3D periodic trajectory, obtained as solution of the OCP, and we parametrize it. Considering a tether with constant length r, the kite moves on the surface of a sphere of radius r, and its position can be defined by the azimuth and elevation angles (ϕ and β, respectively) in spherical coordinates. Thus, our 3D path reduces to a 2D surface path in a (ϕ, β) referential, typically a periodic motion, clockwise, of elliptical shape or figure–of–eight (lemniscate) shape.

2.2 Heading Angle Dynamics

Consider a coordinate system $(\mathbf{e}_1, \mathbf{e}_2, \mathbf{e}_3)$ attached to the kite body, where $\mathbf{e}_1$ is in the kite longitudinal axis pointing forward, $\mathbf{e}_2$ is in the kite transversal axis pointing to the left wing tip, and $\mathbf{e}_3$ is in the kite vertical axis pointing upwards, satisfying $\mathbf{e}_3 = \mathbf{e}_1 \times \mathbf{e}_2$.

We assume the kite aligns naturally with the apparent wind velocity $\mathbf{v}_a$, therefore we can define the kite longitudinal axis to be $\mathbf{e}_1 = -\frac{\mathbf{v}_a}{\|\mathbf{v}_a\|}$. Since the speed of the kite is generally much larger than the wind speed, the apparent wind velocity, and thus the kite longitudinal axis can be considered to be in the plane τ, spanning (ϕ, β), tangent to the sphere centered at the ground station and with radius equal to the tether length.

For a roll angle (ψ) around the longitudinal axis equal to zero, the vector e_3 aligned with the Lift Force is completely

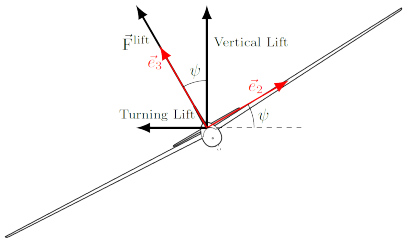

Fig. 2. Roll angle and turning dynamics

radial. As we alter the roll angle, we convey a lateral component to the lift force: the Turning Lift as shown in Figure 2. This Turning Lift causes a lateral acceleration a_l responsible for steering the kite within the tangent plane τ. The lateral acceleration caused by the Turning Lift is given by

$$a_l = \frac{1}{m} \mathrm{F}^{\mathrm{lift}} \sin(\psi). \tag{1}$$

2.3 Guidance Logic

The Guidance Logic used here for the basis controller is the one recently reported in Silva et al. (2019), which is based on a modification of Park et al. (2004) .

We use a reference target approach to follow the path parameterized in (ϕ, β) space. Given the kite current position $\mathbf{p}(\phi, \beta)$, we begin by computing its closest point $(\boldsymbol{Q})$ in the path, defining also the cross–track distance d; see Figure 3. Then, we find the reference point $\boldsymbol{R}$ in the path distancing a given L_0 ahead of $\boldsymbol{Q}$. The vector joining the current kite position and the reference point is defined as $\boldsymbol{L_1}$.

The reference for the heading angle adjustment η can be computed as the angle between the kite velocity $\dot{\boldsymbol{p}}$ and the vector $\boldsymbol{L_1}$. Figure 3 describes the variables used in the Guidance Logic.

We then compute the required centripetal acceleration for the kite to follow a curved line joining the current position at the reference point $\boldsymbol{R}$. This centripetal acceleration is

$$a_s = 2\frac{v^2}{L_1} \sin(\eta), \tag{2}$$

where v is the kite speed, $v = |\dot{\boldsymbol{p}}|$.

This guidance logic differs from the one in Park et al. (2004) since it is the length of L_0 and not of L_1 which is defined a priori. This modification allows a larger domain of attraction since the guidance logic with a fixed L_1 would require that $d < \|L_1\|$ to function properly. With this modification, such condition is always satisfied since L_1 is computed by $L_1 = \sqrt{d^2 + L_0^2}$. (See Silva et al. (2019) for details)

2.4 Heading Angle Control

We act on the roll angle in order to steer the kite. The Heading Angle Control is based on the required centripetal acceleration calculated through equation (2) and the lateral acceleration provided by the Turning Lift, and therefore the roll angle, computed by equation (1). Making both accelerations equal, we can compute the

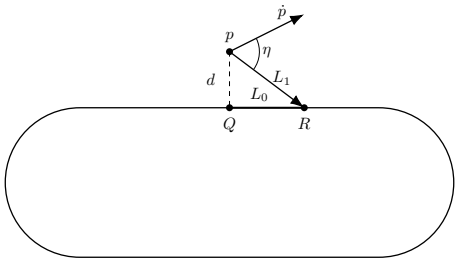

Fig. 3. Guidance logic to follow a reference in the path.

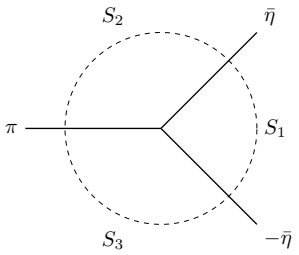

Fig. 4. Domain of attraction regions for the stabilizing controller.

required roll angle to give a trajectory convergent to the path as:

$$\psi = \arcsin\left(2m\frac{v^2\sin(\eta)}{\mathrm{F}^{\mathrm{lift}}L_1}\right). \tag{3}$$

However, having a limited range for the values of the roll angle $\psi \in [-\psi_{\max}, \psi_{\max}]$, the control with saturation is given by:

$$\psi = \min\left\{\psi_{\max}, \max\left\{-\psi_{\max}, \arcsin\left(2m\frac{v^2\sin(\eta)}{\mathrm{F}^{\mathrm{lift}}L_1}\right)\right\}\right\}.$$

Figure 1 shows, in red, a simulation of a trajectory using the guidance control described above for the pre-defined path.

The domain of attraction for our controller without saturation is the set:

$$S_1 := \{(d,\eta) : d \in \mathbb{R}, \eta \in [-\overline{\eta}, \overline{\eta}]\}, \tag{4}$$

where $\overline{\eta}$ is the angle in $(0, \pi/2)$ satisfying $\sin\overline{\eta} = \frac{2mv^2}{\mathrm{F}^{\mathrm{lift}}L_1}\sin\psi_{max}$.

Let S_2 and S_3 be the sets:

$$S_2 := \{(d,\eta) : d \in \mathbb{R}, \eta \in (\overline{\eta}, \pi]\}, \tag{5}$$

$$S_3 := \{(d,\eta) : d \in \mathbb{R}, \eta \in (-\pi, -\overline{\eta})\}. \tag{6}$$

A global domain $S := \{(d,\eta) : d \in \mathbb{R}, \eta \in (-\pi, -\pi]\}$ can be defined as the union of the sets S_1,S_2 and S_3. See Fig. 4.

Finally, we can provide the guidance logic controller that gives the reference for the roll angle $\psi_{ref} = K_{GL}$, which for a given speed v is a function of (d,η)

$$K_{GL}(d,\eta) = \begin{cases} \psi_{\max} & \text{if } (d,\eta) \in S_2, \\ \arcsin\left(\dfrac{2mv^2\sin(\eta)}{\mathrm{F}^{\mathrm{lift}}\sqrt{L_0^2+d^2}}\right) & \text{if } (d,\eta) \in S_1, \\ -\psi_{\max} & \text{if } (d,\eta) \in S_3, \end{cases} \tag{7}$$

This controller has been shown to be asymptotically stabilizing with global domain of attraction S, i.e. the domain of validity of the local dynamical model of the kite (Silva et al., 2019).

3. MODEL PREDICTIVE CONTROL

3.1 Sampled-data Model Predictive Control Framework

Consider a sequence of sampling instants $\pi := \{t_k\}_{k\in\mathbb{N}}$ with a constant sampling period $\delta > 0$ and $t_{i+1} = t_i + \delta$ for all $k \in \mathbb{N}$.

The sampled-data feedback is constructed using an MPC strategy, which involves solving a sequence of open-loop optimal control problems (OCPs) at each sampling instant $t_k \in \pi$, every time using the currently measured state of the plant x_{t_k}. The OCPs $\mathcal{P}(x_{t_k})$ considered are as follows.

$$\begin{aligned} \mathcal{P}(x_{t_k}) : \text{Minimize} \quad & \int_0^T L(x(t),u(t))dt + G(x(T)), \\ \text{subject to} \quad & \dot{x}(t) = f(x(t),u(t)) \text{ a.e.} t \in [0,T], \\ & x(0) = x_{t_k}, \\ & x(t) \in X \qquad \text{all} \quad t \in [0,T], \\ & x(T) \in X_f, \\ & u(t) \in U \qquad \text{a.e.} t \in [0,T]. \end{aligned}$$

The MPC algorithm constructs a sampled-data feedback control by concatenating the initial parts of the optimal control functions obtained as solution to each problem $\mathcal{P}(x_{t_k})$ along each $t_k \in \pi$. Starting at $t_k = t_0$, the following steps are carried out.

1. Measure the current state of the plant x_{t_k}.
2. Solve problem $\mathcal{P}(x_{t_k})$ obtaining the optimal control function $\bar{u} : [t_k, t_k + T] \mapsto \mathbb{R}^m$ (as well as the corresponding trajectory $\bar{x} : [t_k, t_k + T] \mapsto \mathbb{R}^n$).
3. Apply to the plant the control $u^*(t) := \bar{u}(t)$ in the interval $[t_k, t_k + \delta)$ (the remainder of the control function $\bar{u}(t)$, $t > t_k + \delta$ is disregarded).
4. Repeat for the next sampling time $t_k = t_k + \delta$.

The stability guarantees of a sampled-data MPC framework have been studied in Chen and Allgöwer (1998); Fontes (2001); Findeisen and Allgöwer (2002), among others. Following (Fontes, 2001), stability is guaranteed if the design parameters T, L, G and X_f satisfy certain conditions, chief of which is the Lyapunov decrease of the cost functions pair of the OCP, namely the existence of a feedback κ such that

$$\nabla G(x)\cdot f(x,\kappa(x)) \le -L(x,\kappa(x)), \tag{9}$$

with $\kappa(x) \in U$, for all $x \in X_f$.

We show below that this inequality is satisfied for the AWE path-following problem using the feedback control devised in the previous section in the role of κ.

3.2 Model Predictive Control of AWES

Our goal is to guarantee that the trajectory converges to the reference path. This is achieved if the coordinates (d,η), relative to the path, converge to the origin. Alternatively, convergence is also achieved if (d,η_2) converges to the origin, where η_2 is the angle between the current

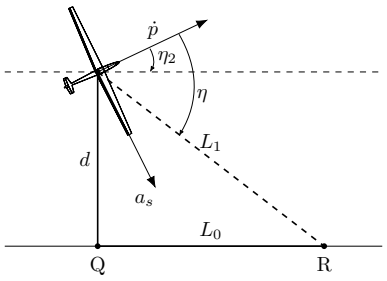

Fig. 5. Motion relative to path in the (d, η) or (d, η_2) coordinates.

velocity vector and the tangent to the desired path at the nearest point (see Fig. 5). Consider the following equations of motion

$$\dot{d} = v \sin \eta_2 \quad \text{and} \quad \dot{\eta}_2 = -\frac{a_s}{v}. \tag{10}$$

Consider also the following lateral acceleration, that corresponds to the control K_{GL} defined in equation (7)

$$a_s(t) = \begin{cases} \dfrac{2v^2}{L_1} \sin(\eta) & \text{if } (d, \eta) \in S_1, \\ \dfrac{2v^2}{L_1} \sin(\bar{\eta}) & \text{if } (d, \eta) \in S_2, \\ -\dfrac{2v^2}{L_1} \sin(\bar{\eta}) & \text{if } (d, \eta) \in S_3, \end{cases} \tag{11}$$

Using this acceleration, it is shown in Silva et al. (2019) that:

(1) when in the regions S_2 and S_3 the states are driven to the region S_1,
(2) the region S_1 is invariant,
(3) within S_1, we can find a Lyapunov function to establish convergence of (d, η_2) to the origin,

which guarantees convergence to the path. The last step used the following Lyapunov function

$$\mathcal{V}(d, \eta_2) = \frac{1}{2} \left(v \sin \eta_2\right)^2 + v^2 \left(\ln \left(L_0^2 + d^2\right) - \ln \left(L^2\right)\right),$$

which has time derivative

$$\dot{\mathcal{V}}(d, \eta_2) = -\frac{2v^3}{L_1} \sin^2 \eta_2 \cos \eta.$$

Now, using MPC on top of the previous stabilizing law, with adequately selected design parameters, preserves the stability for this system. The MPC data used for this specific problem is as follows

$$x = (d, \eta_2), \quad f(x, u) = \left(v \sin \eta_2, -\frac{a_s + u}{v}\right), \tag{12}$$

$$X = S, \quad X_f = S_1, \tag{13}$$

$$G(x) = \mathcal{V}(x), \quad L(x) = \dot{\mathcal{V}}(x), \tag{14}$$

$$U = \{u : u + a_s \in [-\bar{a}_s, +\bar{a}_s]\} \text{ with } \bar{a}_s = \frac{2v^2}{L_1} \sin(\bar{\eta}) \tag{15}$$

For these data, the control $u \equiv 0$ is used as an initial guess and it is a solution to the optimal control problem that stabilizes the system (the feedback (11) is applied to the system). Therefore, solving the optimal control problem can only improve upon the initial guess, considering the objective function as a performance criterion. Since the objective function (running cost $L(\cdot)$ and terminal cost $G(\cdot)$) were selected to form a control Lyapunov pair, the Lyapunov decrease condition (9) is satisfied, and so the MPC framework is stabilizing.

REFERENCES

Chen, H. and Allgöwer, F. (1998). A quasi-infinite horizon nonlinear model predictive control scheme with guaranteed stability. *Automatica*, 34(10), 1205–1217.

De Lellis, M., Saraiva, R., and Trofino, A. (2018). Optimization of Pumping Cycles for Power Kites. In R. Schmehl (ed.), *Airborne Wind Energy: Advances in Technology Development and Research*, 335–359. Springer, Singapore. doi:10.1007/978-981-10-1947-0-14.

Fagiano, L. (2009). *Control of Tethered Airfoils for High–Altitude Wind Energy Generation*. PhD Thesis, Politecnico di Torino.

Findeisen, R. and Allgöwer, F. (2002). An introduction to nonlinear model predictive control. In *21st Benelux meeting on systems and control*, volume 11, 119–141.

Fontes, F.A. (2001). A general framework to design stabilizing nonlinear model predictive controllers. *Systems & Control Letters*, 42(2), 127–143.

Houska, B. and Diehl, M. (2007). Optimal control for power generating kites. In *2007 European Control Conference (ECC)*, 3560–3567. doi: 10.23919/ECC.2007.7068861.

Lellis, M.D., Saraiva, R., and Trofino, A. (2013). Turning angle control of power kites for wind energy. In *52nd IEEE Conference on Decision and Control*, 3493–3498. doi:10.1109/CDC.2013.6760419.

Magni, L., Scattolini, R., and Åström, K. (2002). Global stabilization of the inverted pendulum using model predictive control. *IFAC Proceedings Volumes*, 35(1), 141 – 146. doi:https://doi.org/10.3182/20020721-6-ES-1901.00592. 15th IFAC World Congress.

Paiva, L.T. and Fontes, F.A. (2018). Optimal Control Algorithms with Adaptive Time-Mesh Refinement for Kite Power Systems. *Energies*, 11(3), 475. doi: 10.3390/en11030475.

Park, S., Deyst, J., and How, J. (2004). A New Nonlinear Guidance Logic for Trajectory Tracking. In *AIAA Guidance, Navigation, and Control Conference and Exhibit*. AIAA, Providence, Rhode Island. doi:10.2514/6.2004-4900.

Schmehl, R. (ed.) (2018). *Airborne Wind Energy: Advances in Technology Development and Research*. Green Energy and Technology. Springer Singapore.

Silva, G.B., Paiva, L.T., and Fontes, F.A. (2019). A Path-following Guidance Method for Airborne Wind Energy Systems with Large Domain of Attraction. In *2019 American Control Conference (ACC)*, 2771–2776.

van Hussen, K., Dietrich, E., Smeltink, J., Berentsen, K., van der Sleen, M., Haffner, R., and Fagiano, L. (2018). Study on challenges in the commercialisation of airborne wind energy systems. Technical report, Directorate-General for Research and Innovation, European Commission. Doi: 10.2777/87591.

Zeiaee, A., Soltani-Zarrin, R., Fontes, F.A., and Langari, R. (2017). Constrained directions method for stabilization of mobile robots with input and state constraints. In *2017 American Control Conference (ACC)*, 3706–3711. IEEE.